Perpendicular magnetic anisotropy in Ta/Co2FeAl/MgO multilayers

M. S. Gabor, T. Petrisor, C. Tiusan, and T. Petrisor

Citation: J. Appl. Phys. **114**, 063905 (2013); doi: 10.1063/1.4818326
View online: http://dx.doi.org/10.1063/1.4818326
View Table of Contents: http://jap.aip.org/resource/1/JAPIAU/v114/i6
Published by the AIP Publishing LLC.

Perpendicular magnetic anisotropy in Ta/Co_2FeAl/MgO multilayers

M. S. Gabor,[1,a)] T. Petrisor, Jr.,[1] C. Tiusan,[1,2,b)] and T. Petrisor[1]
[1]*Center for Superconductivity, Spintronics and Surface Science, Technical University of Cluj-Napoca, Cluj-Napoca, Romania*
[2]*Institut Jean Lamour, P2M, CNRS-Nancy University, Nancy, France*

(Received 6 June 2013; accepted 29 July 2013; published online 12 August 2013)

In this paper, we demonstrate the stabilization of perpendicular magnetic anisotropy (PMA) in Ta/Co_2FeAl/MgO multilayers sputtered on thermally oxidized Si(100) substrates. The magnetic analysis points out that these films show significant interfacial anisotropy even in the as-deposited state, $K_S = 0.67\,\mathrm{erg/cm^2}$, enough to provide PMA for the as-deposited films with thicknesses below 1.5 nm. Moreover, the interfacial anisotropy is enhanced by thermal annealing up to 300 °C. The presence of a magnetic dead layer, whose thickness increases with annealing temperature, was also identified. © *2013 AIP Publishing LLC*. [http://dx.doi.org/10.1063/1.4818326]

I. INTRODUCTION

Magnetic tunnel junctions (MTJs) with ferromagnetic electrodes showing perpendicular magnetic anisotropy (PMA) are of great interest since they exhibit several advantages with respect to the MTJs with ferromagnetic electrodes displaying in-plane magnetic anisotropy. They allow the reduction of the spin transfer torque (STT) switching current density (J_{c0})[1,2] due to the absence of the demagnetization term, and show higher stability against thermal fluctuations as a result of their larger anisotropy energy compared to the established in-plane magnetized materials. The conventional PMA materials explored so far include the $L1_0$ ordered alloys (FePt and CoPt), Co-based multilayers (Co/Pd and Co/Pt), and rare-earth and transition metal alloys.[3–9] However, these materials suffer from some limitations including insufficient chemical and/or thermal stability and low spin polarization. Recently, it was shown that CoFeB-MgO interfacial magnetic anisotropy can be used to manufacture MTJs with thin CoFeB layers (<1.5 nm) showing perpendicular magnetic easy axis and which maintain a large magnetoresistive ratio.[10] However, the Gilbert damping constant (α) of CoFeB films was found to increase with decreasing the films thickness[10] and since J_{c0} is proportional to α, this might constitute a disadvantage for STT switching.

A material that seems to be an ideal candidate as a ferromagnetic electrode for perpendicular magnetic tunnel junctions (p-MTJs) is the full Heusler alloy Co_2FeAl (CFA). It was demonstrated to provide giant tunneling magnetoresistance (GTMR) in MgO based MTJs.[11–14] Moreover, this material is of special importance since it was shown to possess a low Gilbert damping,[15–17] essential for applications concerning STT switching. CFA is a material with a relative low cubic magnetic anisotropy,[18] which was found to provide PMA in Pt/CFA/MgO and Cr/CFA/MgO trilayer structures.[19,20] In this paper, we extend these studies and demonstrate the presence of PMA in relatively thick CFA films in Ta/CFA/MgO trilayers. Furthermore, we will show that the CFA films thinner than 1.5 nm exhibit perpendicular magnetic easy axis even before annealing.

II. EXPERIMENTAL

The Si/SiO_2/Ta(6 nm)/CFA(0.9–4.8 nm)/MgO(0.65 nm)/Ta(1.2 nm) multilayer stacks were elaborated using a magnetron sputtering system having a base pressure lower than 4×10^{-9} Torr. The metallic films were deposited at room temperature (RT) by DC sputtering under an Ar pressure of 1 mTorr. For the growth of the CFA layer, a 2-in. Co_2FeAl stoichiometric target was used. The MgO film was grown at RT by rf sputtering from a MgO polycrystalline target in an Ar pressure of 15 mTorr. After deposition, the multilayers were *ex situ* annealed for 1 h at temperatures up to 350 °C in a vacuum better than 3×10^{-8} Torr in the absence of an applied magnetic field. The crystalline structure of the multilayers was analyzed by x-ray diffraction (XRD) using a four-circle diffractometer. The magnetic properties of the films were studied at RT using a Vibrating Sample Magnetometer (VSM).

III. RESULTS AND DISCUSSIONS

In order to determine the crystal structure of the multilayers, we performed x-ray diffraction experiments in grazing incidence geometry (GIXRD). For getting the maximum diffracted signal, our analysis has been performed on the sample with the thicker CFA layer: Ta(6 nm)/CFA(4.8 nm). Figure 1 shows the diffraction pattern recorded for this sample, annealed at 200 °C. In spite of the relative low diffracted signal, the XRD pattern clearly shows peaks corresponding to the Ta (110) and CFA (220), (400), and (422) reflections, respectively. This indicates that at least the CFA film has a polycrystalline structure. After the background subtraction, the diffraction peaks were fitted using pseudo-Voigt functions. This allowed us to evaluate their full width at half maximum (FWHM) and to determine the mean structural coherence length along the grazing direction by means of the well-known Scherrer equation.[21] The obtained values are 1.35 nm for the Ta film and 5.83 nm for the CFA film, respectively. For the samples with thinner CFA films, the XRD analysis is difficult to perform due to the relative low

[a)]Electronic mail: Mihai.Gabor@phys.utcluj.ro
[b)]Electronic mail: Coriolan.Tiusan@phys.utcluj.ro

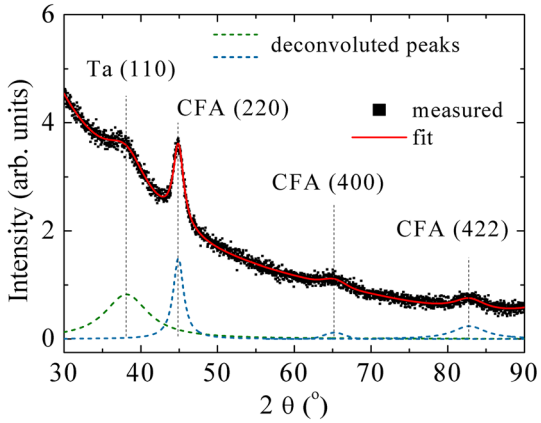

FIG. 1. X-ray diffraction pattern measured in grazing incidence geometry (GIXRD) for the Si/SiO_2/Ta(6 nm)/CFA(4.8 nm)/MgO(0.65 nm)/Ta(1.2 nm) multilayer stack annealed at 200 °C. The symbols represent experimental data, while the lines are the result of the theoretical fit. The vertical dashed lines mark the positions of the Ta(110) and CFA(220), (400), and (422) reflections, respectively.

diffracted signal. However, extrapolating the XRD results obtained for the 4.8 nm thick CFA film sample, it is reasonable to assume that the thinner CFA films are also polycrystalline. This represents a quite different situation with respect to the (100) textured thin films: Fe/MgO(100), CoFeB/MgO(100), and Co_2FeAl/MgO(100) in which PMA has been reported.[10,20,22]

Figure 2 shows in-plane and out-of-plane magnetization curves for the as-deposited and 200 °C annealed samples with CFA thickness of 1.4 and 1.7 nm, respectively. One can observe that the 1.4 nm thick CFA film shows PMA even in the as-deposited state and that the PMA is maintained after annealing. The squareness ratio (M_R/M_S) of the out-of-plane magnetization loop increases from 0.7, before annealing, to 0.9, after annealing. On the other hand, the as-deposited 1.7 nm thick film shows no apparent PMA, while the PMA is clearly achieved after annealing, with an out-of-plane magnetization loop squareness ratio of about 0.7. The origin of PMA at Fe-MgO and Co-MgO interfaces is commonly attributed to the hybridization of the O 2*p* and Co or Fe 3*d*

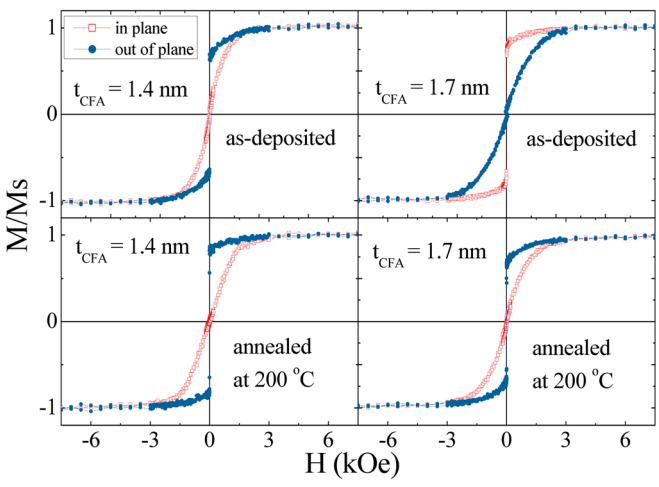

FIG. 2. In-plane and out-of-plane magnetization curves for the as-deposited and 200 °C annealed samples with CFA thickness of 1.4 and 1.7 nm.

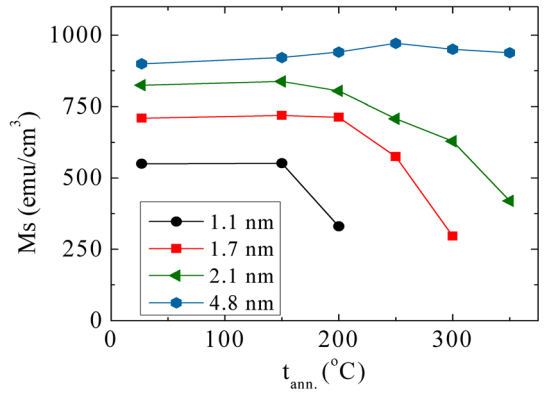

FIG. 3. Evolution of the saturation magnetization (Ms) with the annealing temperature for multilayer stacks with different CFA thicknesses.

orbitals.[22,23] In contrast with previous reports,[19,20] in the case of our samples, the 0.65 nm thick MgO layer seems to provide adequate Co-O and Fe-O bonding at the interface to promote the PMA even before annealing.

To get deeper insight of the role of the annealing on the magnetic properties of the samples, we investigated the evolution of the saturation magnetization (M_S) for CFA films with different thicknesses with respect to the annealing temperature (see Fig. 3). The M_S was determined by taking into account the CFA layers nominal thicknesses. In the case of the 4.8 nm thick film, the Ms shows first a slight increase up to the annealing temperature of 250 °C, and then a small decrease for higher annealing temperatures. In the case of the thinner films, the Ms shows no obvious variation up to an annealing temperature of 150 °C. However, a rather strong decrease of Ms is observed for higher annealing temperatures. Moreover, even for the as-deposited samples, the Ms shows a monotonous reduction with the decrease of the CFA film thickness. These findings give evidence towards a magnetically dead layer present in the CFA films, whose thickness increases with increasing the annealing temperature.

In order to quantify the extent of the magnetic dead layer, we have plotted the M_St vs. t (CFA layer nominal thickness), as shown in Fig. 4(a) for the case of the samples annealed at 150 °C. In this representation, the intercept with the thickness axis of the linear fit of the data gives the magnitude of the dead layer, whereas the slope gives the saturation magnetization (M_S^o) of the CFA film. Our analysis indicates a thickness of the magnetic dead layer (t_{DL}) of around 0.5 nm for annealing temperatures up to 200 °C, which increases up to 1.4 nm for the samples annealed at 350 °C (Fig. 4(b)). This trend is most likely due to the interdiffusion at the CFA-Ta interface, which becomes more pronounced with increasing the annealing temperature. At the same time, the saturation magnetization of the films shows an increase with the annealing temperature, which can be attributed to improvement of the structural quality and of the chemical order with the annealing (Fig. 4(b)).

To quantify the magnitude of the PMA in CFA films, the effective perpendicular magnetic anisotropy constant K_{eff} was determined from the saturation field, H_S, using the relation $K_{eff} = H_S M_S^o/2$. In the case of perpendicular magnetic easy axis, the H_S was considered to be positive and was

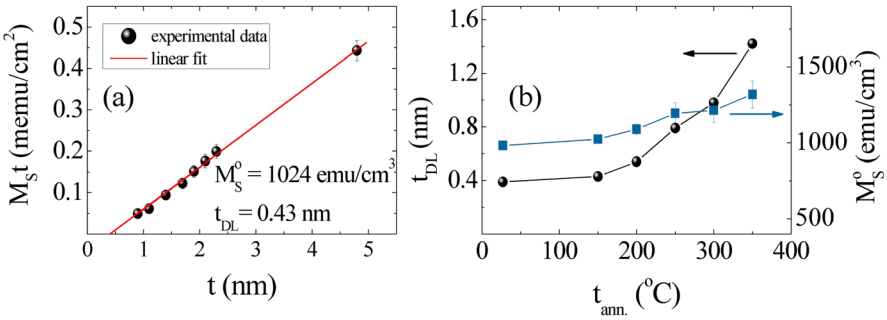

FIG. 4. (a) $M_S t$ vs. CFA nominal layer thickness for the samples annealed at 150 °C. The straight line is the result of the linear fit. (b) Dependence of the magnetic dead layer thickness and saturation magnetization on the annealing temperature.

determined from the in-plane magnetization curve. On the other hand, in the case of in-plane magnetic easy axis, the H_S was considered to be negative and was determined from the out-of-plane hysteresis loop. The K_{eff} can be described by the phenomenological relation[24]

$$K_{eff} = K_v - 2\pi M_S^{o2} + K_S/t_{eff}^{CFA},$$

where K_v describes the bulk magnetocrystalline anisotropy, $2\pi M_S^{o2}$ the shape anisotropy, and K_S the interface anisotropy. By fitting the t_{eff}^{CFA} (CFA layer effective thickness) dependence of the product $K_{eff}t_{eff}^{CFA}$ with the above equation, the different anisotropy contributions can be evaluated. For the films annealed at 150 °C (see Fig. 5), the bulk anisotropy (K_v) was found to be negligible and K_S of about 0.77 erg/cm^2. This value increases to about 1.14 erg/cm^2 if, when deriving the K_S, the nominal thickness of the CFA layer is used instead of the effective one. The K_S for the as-deposited samples was estimated to about 0.67 erg/cm^2. An increase in 0.77–0.95 erg/cm^2 range was observed with increasing the annealing temperature up to 300 °C. This can be related to an improvement of the CFA-MgO interface quality with annealing. At an annealing temperature of 350 °C, the K_S shows a sharp decrease down to about 0.48 erg/cm^2, most likely due to the CFA-Ta enhanced interdiffusion and to the degradation of the thin MgO layer at the upper CFA interface.

Figure 6 shows a contour plot, deduced from the experimental data points, of the $K_{eff}t_{nom.}^{CFA}$ product vs. the nominal thickness of the CFA layer and the annealing temperature. The critical CFA layer thickness, which separates the out-of-plane of the in-plane anisotropy, is situated around 1.5 nm for the as-deposited samples and for the samples annealed at 150 °C. This critical thickness increases to about 1.9 nm for the samples annealed up to 300 °C. This increase is the result of two phenomena: first, the enhancement of the K_S, and second the reduction of the t_{eff}^{CFA} with increasing the annealing temperature. For the samples annealed at 350 °C due to the decrease of K_S and to the increase of the magnetic dead layer thickness (Fig. 4(b)) the CFA thickness range in which one can obtain films with PMA becomes extremely narrow, not suitable for practical purposes related to potential applications of CFA.

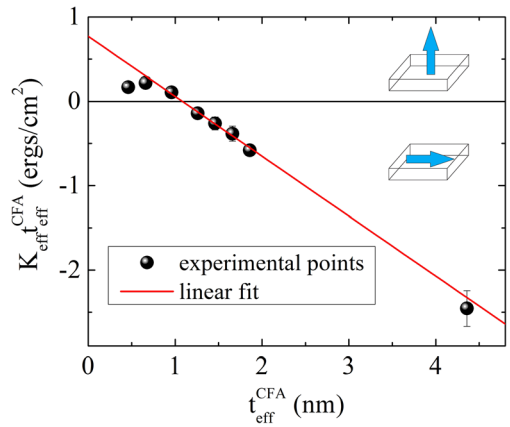

FIG. 5. Dependence of the $K_{eff}t_{eff}^{CFA}$ product on the t_{eff}^{CFA} for the samples annealed at 150 °C. The straight line is the result of a linear fit.

IV. CONCLUSION

We have experimentally demonstrated the stabilization of PMA in Ta/CFA/MgO multilayer stacks grown by sputtering on thermally oxidized Si(100) substrates. Our CFA layers show significant interfacial anisotropy, $K_S = 0.67$ erg/cm^2, even in the as-deposited state. This is sufficient to provide PMA for as deposited magnetic films with thickness below 1.5 nm. An increase of K_S in the 0.77-0.95 erg/cm^2 range was observed with increasing the annealing temperature up to 300 °C. The presence of a magnetic dead layer, whose thickness increases with annealing temperature was also identified. The occurrence of PMA in the as-deposited samples renders the Ta/Co_2FeAl/MgO system promising from an application point of view.

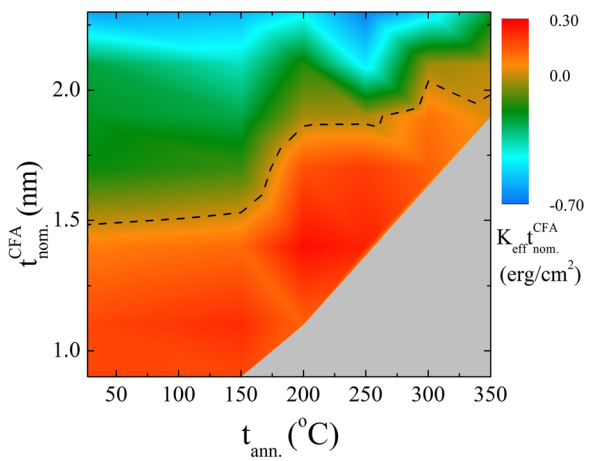

FIG. 6. Contour plot of the $K_{eff}t_{nom.}^{CFA}$ product vs. the nominal thickness of the CFA layer and the annealing temperature. The dashed line depicts the boundary between the in-plane and out-of-plane anisotropy. The gray area is the region where the clear ferromagnetic signal of the CFA films is lost.

ACKNOWLEDGMENTS

This work has been partially supported by CNCSIS UEFISCSU, Project No. PNII IDEI No.4/2010, code ID-106 and by POS CCE ID. 574, code SMIS-CSNR 12467.

[1]S. Yakata, H. Kubota, Y. Suzuki, K. Yakushiji, A. Fukushima, S. Yuasa, and K. Ando, J. Appl. Phys. **105**, 07D131 (2009).
[2]S. Mangin, D. Ravelosona, J. A. Katine, M. J. Carey, B. D. Terris, and E. E. Fullerton, Nature Mater. **5**, 210–215 (2006).
[3]N. Nishimura, T. Hirai, A. Koganei, T. Ikeda, K. Okano, Y. Sekiguchi, and Y. Osada, J. Appl. Phys. **91**, 5246–5249 (2002).
[4]H. Ohmori, T. Hatori, and S. Nakagawa, J. Appl. Phys. **103**, 07A911 (2008).
[5]G. Kim, Y. Sakuraba, M. Oogane, Y. Ando, and T. Miyazaki, Appl. Phys. Lett. **92**, 172502 (2008).
[6]K. Yakushiji, T. Saruya, H. Kubota, A. Fukushima, T. Nagahama, S. Yuasa, and K. Ando, Appl. Phys. Lett. **97**, 232508 (2010).
[7]J.-H. Park, C. Park, T. Jeong, M. T. Moneck, N. T. Nufer, and J.-G. Zhu, J. Appl. Phys. **103**, 07A917 (2008).
[8]B. Carvello, C. Ducruet, B. Rodmacq, S. Auffret, E. Gautier, G. Gaudin, and B. Dieny, Appl. Phys. Lett. **92**, 102508 (2008).
[9]A. Barman, S. Wang, O. Hellwig, A. Berger, E. E. Fullerton, and H. Schmidt, J. Appl. Phys. **101**, 09D102 (2007).
[10]S. Ikeda, K. Miura, H. Yamamoto, K. Mizunuma, H. D. Gan, M. Endo, S. Kanai, J. Hayakawa, F. Matsukura, and H. Ohno, Nature Mater. **9**, 721–724 (2010).
[11]W. Wang, H. Sukegawa, R. Shan, S. Mitani, and K. Inomata, Appl. Phys. Lett. **95**, 182502 (2009).
[12]W. Wang, E. Liu, M. Kodzuka, H. Sukegawa, M. Wojcik, E. Jedryka, G. H. Wu, K. Inomata, S. Mitani, and K. Hono, Phys. Rev. B **81**, 140402 (2010).
[13]W. Wang, H. Sukegawa, and K. Inomata, Phys. Rev. B **82**, 092402 (2010).
[14]Z. Wen, H. Sukegawa, S. Mitani, and K. Inomata, Appl. Phys. Lett. **98**, 192505 (2011).
[15]S. Mizukami, D. Watanabe, M. Oogane, Y. Ando, Y. Miura, M. Shirai, and T. Miyazaki, J. Appl. Phys. **105**, 07D306 (2009).
[16]G. Ortiz, M. S. Gabor, T. Petrisor, Jr., F. Boust, F. Issac, C. Tiusan, M. Hehn, and J. F. Bobo, J. Appl. Phys. **109**, 07D324 (2011).
[17]M. Belmeguenai, H. Tuzcuoglu, M. S. Gabor, T. Petrisor, C. Tiusan, D. Berling, F. Zighem, T. Chauveau, S. M. Chérif, and P. Moch, Phys. Rev. B **87**, 184431 (2013).
[18]M. S. Gabor, T. Petrisor, Jr., C. Tiusan, M. Hehn, and T. Petrisor, Phys. Rev. B **84**, 134413 (2011).
[19]X. Li, S. Yin, Y. Liu, D. Zhang, X. Xu, J. Miao, and Y. Jiang, Appl. Phys. Express **4**, 043006 (2011).
[20]Z. Wen, H. Sukegawa, S. Mitani, and K. Inomata, Appl. Phys. Lett. **98**, 242507 (2011).
[21]A. L. Patterson, Phys. Rev. **56**, 978–982 (1939).
[22]H. X. Yang, M. Chshiev, B. Dieny, J. H. Lee, A. Manchon, and K. H. Shin, Phys. Rev. B **84**, 054401 (2011).
[23]A. Manchon, C. Ducruet, L. Lombard, S. Auffret, B. Rodmacq, B. Dieny, S. Pizzini, J. Vogel, V. Uhlíř, M. Hochstrasser, and G. Panaccione, J. Appl. Phys. **104**, 043914 (2008).
[24]C. A. F. Vaz, J. A. C. Bland, and G. Lauhoff, Rep. Prog. Phys. **71**, 056501 (2008).